VNU Journal of Science: Mathematics – Physics, Vol. 39, No. 2 (2023) 1-14

VNU Journal of Science: Mathematics - Physics

Journal homepage: https://js.vnu.edu.vn/MaP

Original Article

Geometries, Electronic Structures, and Energetic Parameters of the First-row Transition Metal Doped Aluminum Clusters $Al_{16}M$

Hoang Trung Kien[1], Ngo Tuan Cuong[1,*], Nguyen Minh Tam[2]

[1]*Hanoi National University of Education, 136 Xuan Thuy, Cau Giay, Hanoi, Vietnam*

[2]*Ton Duc Thang University, 19 Nguyen Huu Tho, Tan Phong, District 7, Ho Chi Minh City, Vietnam*

Received 10 September 2022
Revised 24 November 2022; Accepted 26 December 2022

Abstract: Using quantum chemical approaches, the geometry, stability, electronic structure, and magnetic property of neutral $Al_{16}M$ clusters with M being a first-row 3*d* transition metal atom, including Sc, Ti, V, Cr, Mn, Fe, Co, Ni, Cu, and Zn were investigated in this work. The neutral $Al_{16}M$ clusters favor three kind of structures based on pure Al_{17} framework, including two exohedral doped isomers and one endohedral doped structure. There is a competition between the endohedral and the exohedral structures of $Al_{16}M$ with M being Ni, Cu, and Zn. The thermodynamic stability of encapsulated structure $Al_{16}Ni$ is confirmed by the calculated average binding energy and embedded energy values. DFT calculation, however, indicate that the doping with transition metals has reduced the ionization potential of the pure aluminum clusters. Based on NBO calculations, a comprehensive picture of magnetic behavior is shown for $Al_{16}M$ clusters. Remarkably, the magnetism of the encapsulated Ni dopant is quenched in Al_{16} cage. Moreover, NBO calculations found that the 50-electron shells are completely preserved in both clusters $Al_{16}Sc$ and $Al_{16}Ti$ and the remaining unpaired electron(s) localize(s) mainly on 3*d* atomic orbitals of the transition metal dopant.

Keywords: Density functional theory calculation, Transition metal doped aluminum cluster, $Al_{16}M$, Electronic structure.

* Corresponding author.
E-mail address: cuongnt@hnue.edu.vn

https//doi.org/10.25073/2588-1124/vnumap.4775

1. Introduction

Due to the properties of atomic clusters not only are markedly different from those of discrete molecules or from large materials, but also change as the size and charge of the atomic clusters change, the study of the correlation between the structure of clusters and the size and charge of the atomic clusters is a prerequisite for understanding their special physical and chemical properties. During the past three decades, theoretical as well as experimental studies on clusters, especially metal clusters to find out their geometrical, electronic, optical, and magnetic properties are still ongoing [1-5].

Aluminum clusters have been intensively studied both for fundamental science and towards application to many technological applications [6, 7]. Along with many experimental investigations on aluminum clusters [8], the theoretical studies of geometrical and electronic structures have been also carried out simultaneously using various theoretical calculation methods. For example, Chuang et al., [9] studied the structure of Al_n clusters (n = 2–23) to demonstrate the ability of the atoms in the cluster to be strongly bonded and the relative stability was evaluated for all clusters of different sizes. Rao et al., [10] reported the stable geometries of neutral, cationic and anionic Al clusters containing up to 15 atoms. The electronic structures, binding energies, relative stability, fragmentation channels, and ionization energies were studied afterwards.

Since doping a hetero element has been indicated as an effective way to improve stability, chemical reactivity, and electronic properties of atomic clusters, many doped aluminum clusters have been investigated both theoretically and experimentally, such as $Al_{12}X$, with X = B, Al, Ga, C, Si, Ge) [11] and $Al_nSi_m^{0/+}$ (with n = 3–16 and m = 1, 2) [12], Al_nM (M = Cr, Mn, Fe, Co, Ni; n = 1–7, 12) [13-17]. In addition, some bimetallic clusters or their ionic states, such as MAl_4^- (M = Li, Na, Cu) and XAl_3^- (X = Si, Ge, Sn, Pb) exhibit the aromatic property [18, 19] and this extends the concept of aromaticity to metal clusters. The magnetism and stability of metal clusters can be tuned by doping transition metal elements, which are characterized by a partially filled *d* shell [20-24]. It is thus expected that transition metal doping into aluminum clusters will yield clusters possessing the novel physico-chemical properties. Many investigations have been carried out on transition metal-doped aluminum clusters and the considerable results have been obtained. Some previous investigations showed that an icosahedral structure can be constructed by twelve aluminum atoms plus a transition metal atom such as Co, Ni, Cu, and Zn in which the atomic radius of the Cu and Zn seems small enough to allow its position at the center of such a cage [13, 25-27]. Particularly, Kumar and Kawazoe [27] performed a study using density functional theory (DFT) calculations on a doping of a copper atom into Al_{12} cluster and discovered a perfect icosahedral $Cu@Al_{12}$ having a high spin state with a 3 μB spin magnetic moment. A combined theoretical and experimental investigation on Al_nV clusters indicated that the anionic $Al_{12}V^-$ favors a distorted icosahedral shape in which the vanadium atom occupies a convex capped site [28]. In an experimental study, Lang et al., [29] found that the cationic transition metal doped aluminum clusters Al_nM^+ attach one argon atom up to a critical cluster size n_{crit}, with n_{crit} = 16 for M = V, Cr, and n_{crit} = 19 – 21 for M = Ti, and undergo a geometrical transition in going from exohedrally to endohedrally doped clusters in which the M atom is located inside an Al cage. These experimental results were then confirmed by subsequent theoretical studies on Al_nV, Al_nTi, and Al_nCr clusters using DFT calculations [30-32]. Recently, a theoretical investigation on the 13-atom clusters Al_xSc_y, with x + y = 13, revealed that both anionic and neutral isomers of Al_xSc_y retain an icosahedral shape of both Al_{13} and Sc_{13} and the spin magnetic moment of Al_xSc_y tends to gradually increase with an increasing number of Sc atoms [33].

Although many investigations on transition metal doped aluminum clusters were performed, however, the geometric and electronic structures of these clusters with the size larger 15 atoms as well as their correlation between their sizes and their physico-chemical properties have not been elucidated so far. Specifically, the studies on Al_{16} doped transition metals $Al_{16}M$ have been limited and scattered.

Consequently, the influence of the doping elements on their geometric structures and absorption spectroscopic properties has been still questionably. Regarding the $Al_{16}M$ atomic cluster, with the number of valence electrons of 16 Al atoms being 48, the doping of an 3*d* transition metal atom will make the total number of electrons of the clusters close to the magic number 50. Moreover, the energetic parameters such as binding energy and dissociation energy of these clusters also needs to be elucidated.

In this context, by using both density functional theory and wavefunction methods, we set out to perform a systematic theoretical investigation on the geometries, stability, and magnetic properties of the aluminum clusters doped by one 3*d* row transition metal atom in neutral clusters $Al_{16}M$ and their corresponding cationic states, with M going from Sc to Zn. The geometries of the most stable equilibrium structures are thoroughly determined and thereby their structural evolution is explored as well as their electronic configurations, energetic parameters and magnetic properties are assigned.

2. Computational Method

All standard electronic structure calculations are performed using the GAUSSIAN 09 package [34]. A previous theoretical study of Schultz et al., [35] on small pure aluminum clusters showed that for Al_2 and Al_3 clusters, the optimized bond length values and calculated atomization energies obtained at B3LYP/6-31+G (d) level agree well with those at the high accurate calculation level CCSD(T)/6-31+G(d) and experimental values. Moreover, a later study of Ouyang et al., on AlX dimers, with X being 3d, 4d, and 5d transition metal, indicated that the bond length, harmonic vibrational frequency, and dissociation energy calculated at DFT method using B3LYP functional are in good agreement with the available experimental data [36]. Recent studies on aluminum-based clusters have also demonstrated the reliability of the B3LYP functional [12, 34]. Therefore, we select the hybrid B3LYP functional in conjunction with the 6-31+G(d) basis set for all geometrical optimizations as well as subsequently electronic structure calculations. The search for possible structures of clusters is conducted using two different approaches. First, initial structures of each $Al_{16}M$ are manually designed by adding the metal dopant M at all possible positions on the surfaces of the lower-lying Al_{16} isomers reported. By second way, all possible structures of $Al_{16}M$ clusters are generated using a stochastic algorithm [37] which was improved based on the random kick procedure reported by Saunders [38]. The initial guess structures are then geometrically optimized using the same B3LYP functional in conjugation with the small LANL2DZ basis set. 2000 initial structures are randomly generated by using this stochastic algorithm then optimized at the low level B3LYP/LANL2DZ. The most stable structures obtained at this computed level are re-used as input to generate new and further optimized structures. If no new structures are found after within 20 consecutive circles, it can be considered to have converged and the final most stable structures are used as inputs for optimization at higher level B3LYP/6-31+g(d). The local energy minima which are obtained by both approaches and having relative energies of < 3 eV are then reoptimized at different spin states using the same functional but with the larger 6-31+G(d) basis set. Harmonic vibrational frequencies along with zero-point energy (ZPE) corrections of the $Al_{16}M$ clusters are subsequently obtained at the same level. The values of relative energy are determined from B3PW91/6-311+G(d) + ZPE computations.

Moreover, in order to examine the electronic configuration and thereby rationalize the magnetic and chemical bonding properties of the studied clusters, the natural bonding orbital (NBO) analyses are performed by using the NBO 3.0 program also implemented in the Gaussian package. Based on the NBO analyses, the magnetic moments including the total (TMMs) and local (LMMs) values are defined as the difference between the numbers of spin-up and spin-down electrons occupying the molecular/atomic orbitals of the cluster/atom.

3. Result and Discussion

3.1. Geometrical Structures of the Clusters

Shapes of equilibrium structures of $Al_{16}M$ clusters, their spin states, and relative energies obtained at B3LYP/6-31+G(d) are shown in Fig. 1. Due to a large number of isomers located on the potential energy surfaces of the clusters considered, only the low-lying isomers whose relative energies are close to the corresponding most stable structure are presented for each $Al_{16}M$ clusters.

Conventionally, $Al_{16}M.x$ label is used to denote the isomers considered, in which M = Sc, Ti, V, Cr, Mn, Fe, Co, Ni, Cu, and Zn stands for transition metal dopants, and x = A, B, C, etc. refers to the different isomers with increasing relative energy.

The main characteristics of the geometrical features can briefly be summarized as follows:

For $Al_{16}Sc$, both most stable isomers $Al_{16}Sc.A$ and $Al_{16}Sc.B$ exist at doublet spin state and are formed by substituting a Sc atom into a position of Al atom in the neutral Al_{17} framework, [39] which is constructed by capping of four Al atoms on different exohedral positions of the well-known icosahedron Al_{13} [40]. In details, the most stable structure $Al_{16}Sc.A$, in which a vertex Al atom of icosahedral Al_{13} core is substituted by scandium dopant, is 0.29 eV lower in energy than the second isomer $Al_{16}Sc.B$, composed by capping three Al atoms and one Sc atom on exohedral positions of icosahedron Al_{13}.

For $Al_{16}Ti$, form DFT calculations it is found that the structures of $Al_{16}Ti.A$ and $Al_{16}Ti.B$ are stable in a triplet spin state and similar to structures of $Al_{16}Sc.A$ and $Al_{16}Sc.B$, respectively, in which the Sc dopant is substituted by Ti atom. Both structures, however, are degenerate within a tiny energy gap of only 0.07 eV. The structure $Al_{16}Ti.C$, having the closed-shell electronic configuration, is next isomer with the value of relative energy being 0.44 eV.

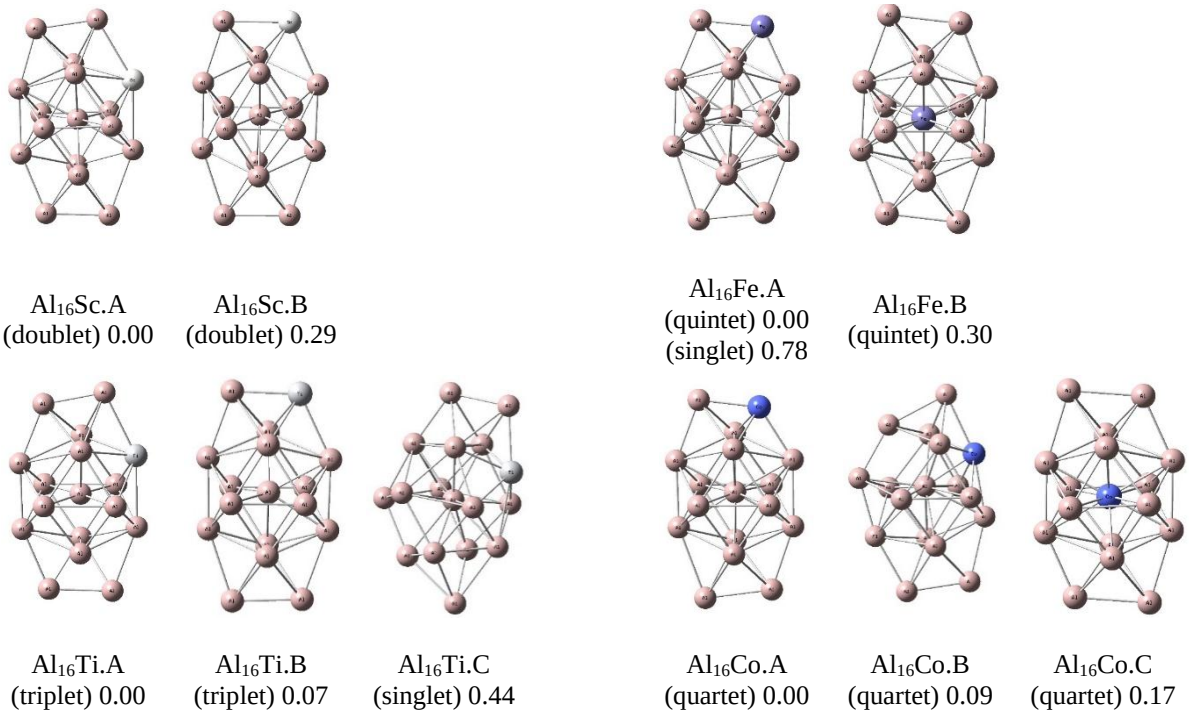

$Al_{16}Sc.A$ (doublet) 0.00 $Al_{16}Sc.B$ (doublet) 0.29 $Al_{16}Fe.A$ (quintet) 0.00 (singlet) 0.78 $Al_{16}Fe.B$ (quintet) 0.30

$Al_{16}Ti.A$ (triplet) 0.00 $Al_{16}Ti.B$ (triplet) 0.07 $Al_{16}Ti.C$ (singlet) 0.44 $Al_{16}Co.A$ (quartet) 0.00 $Al_{16}Co.B$ (quartet) 0.09 $Al_{16}Co.C$ (quartet) 0.17

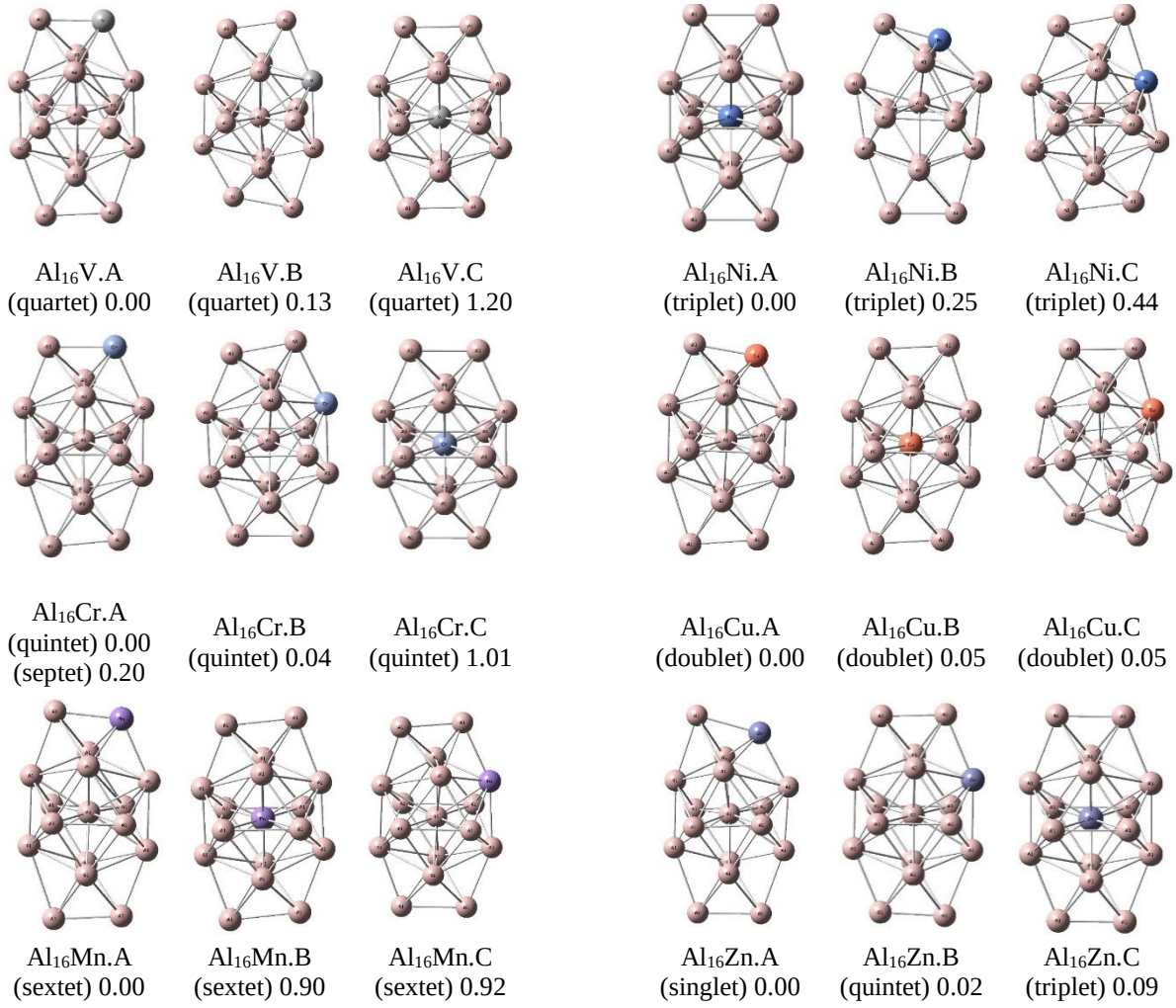

Figure 1. Geometry, relative energy, and spin state (in the bracket) of the most stable isomers $Al_{16}M^{0/-}$, with M = Sc, Ti, V, Cr, Mn, Fe, Co, Ni, Cu, and Zn obtained at (U)B3LYP/6-31+G(d) + ZPE optimizations.

For $Al_{16}Mn$, the lowest-lying isomers of $Al_{16}Mn$ are found to possess a high total magnetic moment of 5 μB, corresponding to sextet spin state. The most stable isomer of $Al_{16}Mn$, $Al_{16}Mn.A$, remains the same geometrical structure as that of $Al_{16}V$ and $Al_{16}Cr$. However, the endohedral structure $Al_{16}Mn.B$, become the second lowest-lying isomer despite of a large relative energy gap of 0.90 eV.

For $Al_{16}Fe$, both the most stable isomers $Al_{16}Fe.A$ and $Al_{16}Fe.B$ are similarly to $Al_{16}Mn.A$ and $Al_{16}Mn.B$, respectively, but with smaller relative energy gap, being 0.3 eV, and lower magnetic moment of 4 μB, corresponding to quintet spin state.

For $Al_{16}Co$, according to DFT calculations, both the most stable structures $Al_{16}Co.A$ and $Al_{16}Co.B$ are degenerate within a tiny energy gap of 0.09 eV. The lowest-lying isomer $Al_{16}Co.A$ still keep the structure that is formed similarly to $Al_{16}M$, with M being V, Cr, and Mn. The endohedral structure $Al_{16}Co.C$ is the next isomer with a relative energy gap of 0.17 eV higher in energy than $Al_{16}Co.A$. Besides, all presented structures exist at quartet spin state.

For $Al_{16}Ni$, remarkably, $Al_{16}Ni$ prefers the endohedral structure $Al_{16}Ni.A$ at triplet spin state as the most stable structure. Two next isomers $Al_{16}Ni.A$ and $Al_{16}Ni.B$, also existing at triplet spin state, is 0.25 eV and 0.44 eV higher in energy than $Al_{16}Co.A$, respectively.

For $Al_{16}Cu$, it is found that a structure competition among three isomers having doublet spin state, including an endohedrally doped structure $Al_{16}Cu.B$ and two exohedrally doped structures $Al_{16}Cu.A$ and $Al_{16}Cu.C$, with tiny energy gap of only 0.05 eV.

For $Al_{16}Zn$, similarly, to $Al_{16}Cu$, DFT calculations result again in energetic degeneracies of the three lowest-lying isomers, with energy gaps < 0.1 eV. The exohedral structure $Al_{16}Zn.A$, having the same shape as the most stable structures of others $Al_{16}M$, with M being V, Cr, Mn, Fe, Co, and Cu, is only 0.02 eV lower in energy than another exohedral isomer $Al_{16}Zn.B$ and 0.09 eV lower in energy than the endohedral isomer $Al_{16}Zn.C$. All these isomers are stable with closed-shell electronic configuration.

In general, it is found that the neutral $Al_{16}M$, with M being a transition metal atom and going from Sc to Zn, are stabilized at three kind of structures, including two exohedral doped isomers and one endohedral doped structure. When M goes from Ni to Zn, there is a competition between the endohedral and the exohedral structures as shown by the fact that the most stable isomer of $Al_{16}Ni$ favors endohedral shape while the relative energy gaps between the endohedral and the exohedral structures for both $Al_{16}Cu$ and $Al_{16}Zn$ are lower than 0.1 eV.

3.2. Energetic Parameters

To evaluate the thermodynamic stability, the average binding energies (E_b) of the considered clusters are determined and compared to that of the relevant pure aluminum clusters Al_{17}. The E_b values of the $Al_{16}M$ clusters can be defined in Eq. (1)

$$E_b(Al_{16}M) = [16E(Al) + E(M) – E(Al_{16}M)]/17 \quad (1)$$

where E(Al), and E(M), are the total energies of the Al-atom and the M-atom, respectively, and $E(Al_{16}M)$ are the total energies of the neutral $Al_{16}M$.

Similarly, for the neutral Al_{17}, the E_b can be defined by Eq. (2) as follows:

$$E_b(Al_{17}) = [17E(Al) – E(Al_{17})]/17 \quad (2)$$

Table 1. The energetic paprameters of $Al_{16}M$ cluster, including a) Average binding energy, b) Embedded energy, and c) Ionization energy of $Al_{16}M$ clusters

a) Average binding energy, E_b (eV)		b) Embedded energy, E_e (eV)		c) Ionization energy, IE (eV)	
$Al_{16}Sc$	2.08	$Al_{16}Sc \rightarrow Al_{16} + Sc$	2.80	$Al_{16}Sc \rightarrow Al_{16}Sc^+$	5.50
$Al_{16}Ti$	2.09	$Al_{16}Ti \rightarrow Al_{16} + Ti$	2.93	$Al_{16}Ti \rightarrow Al_{16}Ti^+$	5.63
$Al_{16}V$	2.07	$Al_{16}V \rightarrow Al_{16} + V$	2.61	$Al_{16}V \rightarrow Al_{16}V^+$	5.58
$Al_{16}Cr$	2.02	$Al_{16}Cr \rightarrow Al_{16} + Cr$	1.85	$Al_{16}Cr \rightarrow Al_{16}Cr^+$	5.55
$Al_{16}Mn$	2.00	$Al_{16}Mn \rightarrow Al_{16} + Mn$	1.49	$Al_{16}Mn \rightarrow Al_{16}Mn^+$	5.48
$Al_{16}Fe$	2.08	$Al_{16}Fe \rightarrow Al_{16} + Fe$	2.73	$Al_{16}Fe \rightarrow Al_{16}Fe^+$	5.37
$Al_{16}Co$	2.06	$Al_{16}Co \rightarrow Al_{16} + Co$	2.53	$Al_{16}Co \rightarrow Al_{16}Co^+$	5.45
$Al_{16}Ni$	2.10	$Al_{16}Ni \rightarrow Al_{16} + Ni$	2.94	$Al_{16}Ni \rightarrow Al_{16}Ni^+$	5.61
$Al_{16}Cu$	2.05	$Al_{16}Cu \rightarrow Al_{16} + Cu$	2.30	$Al_{16}Cu \rightarrow Al_{16}Cu^+$	5.51
$Al_{16}Zn$	1.94	$Al_{16}Zn \rightarrow Al_{16} + Zn$	0.33	$Al_{16}Zn \rightarrow Al_{16}Zn^+$	5.62
Al_{17}	2.04	$Al_{17} \rightarrow Al_{16} + Al$	2.14	$Al_{17} \rightarrow Al_{17}^+$	5.65

All these energy values are obtained from B3LYP/6-31+G(d) + ZPE calculations and displayed in Table 1 while the plots of E_b depicted Fig. 2a illustrate their evolution. The trends of E_b values in neutral $Al_{16}M$ are quite similar to each other. In comparison to the E_b value of Al_{17}, the E_b values of $Al_{16}M$ are higher when the M dopant goes from Sc to V, then decrease to lower values with M being Cr and Mn. As M goes from Fe to Cu, the E_b values of $Al_{16}M$ return to be higher than that of Al_{17} before decreasing to the lowest E_b value at $Al_{16}Zn$. These calculated results prove that a doping of the first-row transition metal M, except for Cr, Mn, and Zn, into Al_{16} enhances the cluster stability as compared to the pure aluminum Al_{17} clusters. Remarkably, the endohedral structure $Al_{16}Ni$ in which Ni dopant is encapsulated at the centre of aluminum cage Al_{16}, reveal the highest E_b value as compared to the remaining $Al_{16}M$ counterparts.

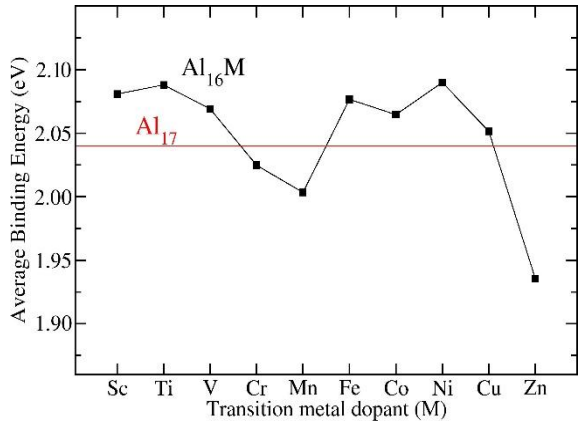

a) The average binding energy of $Al_{16}M$ clusters

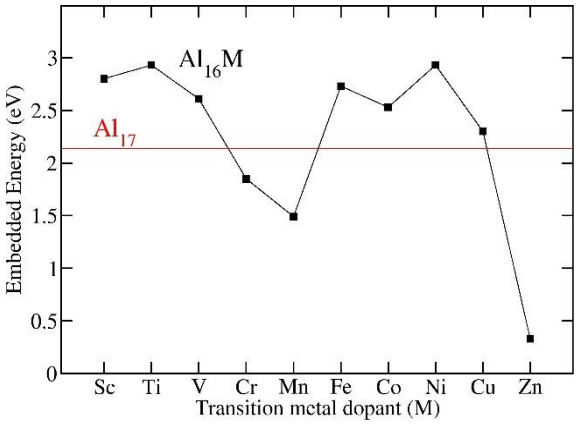

b) The embedded energy of $Al_{16}M$ clusters

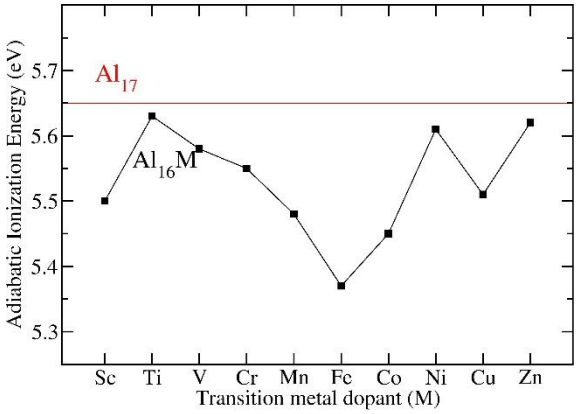

c) The adiabatic ionization energy of $Al_{16}M$ clusters

Figure 2. Evolution of the average binding energy, embedded energy, and adiabatic ionization energy of the $Al_{16}M$ clusters considered. Values are obtained from (U)B3PW91/6-31+G(d) + ZPE computations.

To support the above findings, the embedded energy (*EE*) of the most stable isomers of $Al_{16}M$ clusters are further examined. The embedded energy is defined as the energy gained in incorporating a

M-dopant into the Al_{16} hosts. In the other words, the embedded energy of $Al_{16}M$ is the dissociation energy of the neutral Al_{16} for the M impurity atom elimination. The embedded energy (E_e) is defined by Eq. (3):

$$E_e(Al_{16}M) = E(Al_{16}) + E(M) - E(Al_{16}M) \quad (3)$$

where $E(Al_{16})$ and $E(M)$ are the total DFT energies of the neutral Al_{16} clusters and transition metal atom M, respectively. The total energies of Al_{16} and M are calculated for the ground states of the pure neutral cluster Al_{l6} which were previously reported [38] and which spin state at which M metal atom is stabilized, respectively. The E_e values of $Al_{16}M$, obtained at the same DFT calculating level and displayed on Table 1b and Fig. 2b. According to DFT calculations, the E_e and E_b values of $Al_{16}M$ have the same trend. Similarly, to E_b values, in comparison to the E_e value of Al_{17}, the E_e value of $Al_{16}M$ is higher with the M being Sc, Ti, V, Fe, Co, Ni and Cu whereas it is lower with M being Cr, Mn and gets the minimum value at M = Zn. The E_e gets the maximum value of 2.93 eV at M = Ti and M = Ni. This once again confirms the thermodynamic stability of the endohedrally doped structure $Al_{16}Ni$.

In addition to the average binding energy and the embedded energy of the $Al_{16}M$ clusters, their adiabatic ionization energies (AIEs) are also examined at the same DFT level presented in Table 1c and Fig. 3. The AIE is calculated as the difference of the electronic energies, corrected by ZPEs, of each neutral isomer of $Al_{16}M$ and its corresponding cation having the similar shape. DFT calculations indicate that the AIE values of $Al_{16}M$ clusters range from 5.37 to 5.63, corresponding to the lowest value at M = Fe and the highest at M = Ti. However, all these values are less than 5.65 eV, which is the AIE value of the Al_{17} cluster. This proves that the transition metal doping reduces the ionization potential of the pure aluminum clusters.

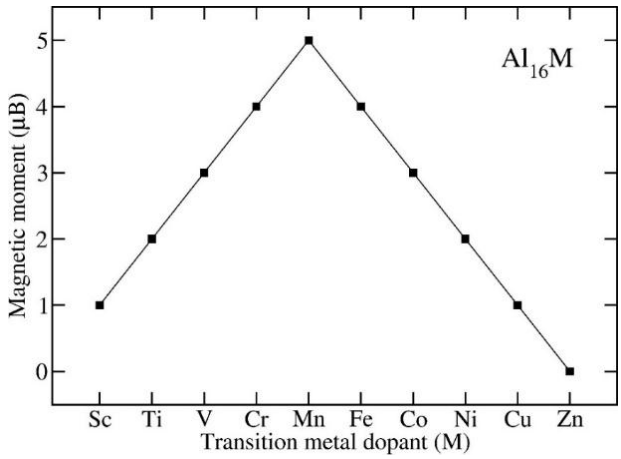

Figure 3. Evolution of total magnetic moment (μB) of $Al_{16}M$.

3.3. Electronic Structure of the Clusters

In order to investigate the electronic structures of the most stable isomers of the $Al_{16}M$ clusters, with M from Sc to Zn, we continue to use DFT method employing the B3LYP/6-31+G(d) functional and basis set to perform NBO calculations. From results of the calculations, the images of several frontier orbitals of the $Al_{16}Sc$ cluster are plotted as a representative for the inspection, as shown in Fig. 4.

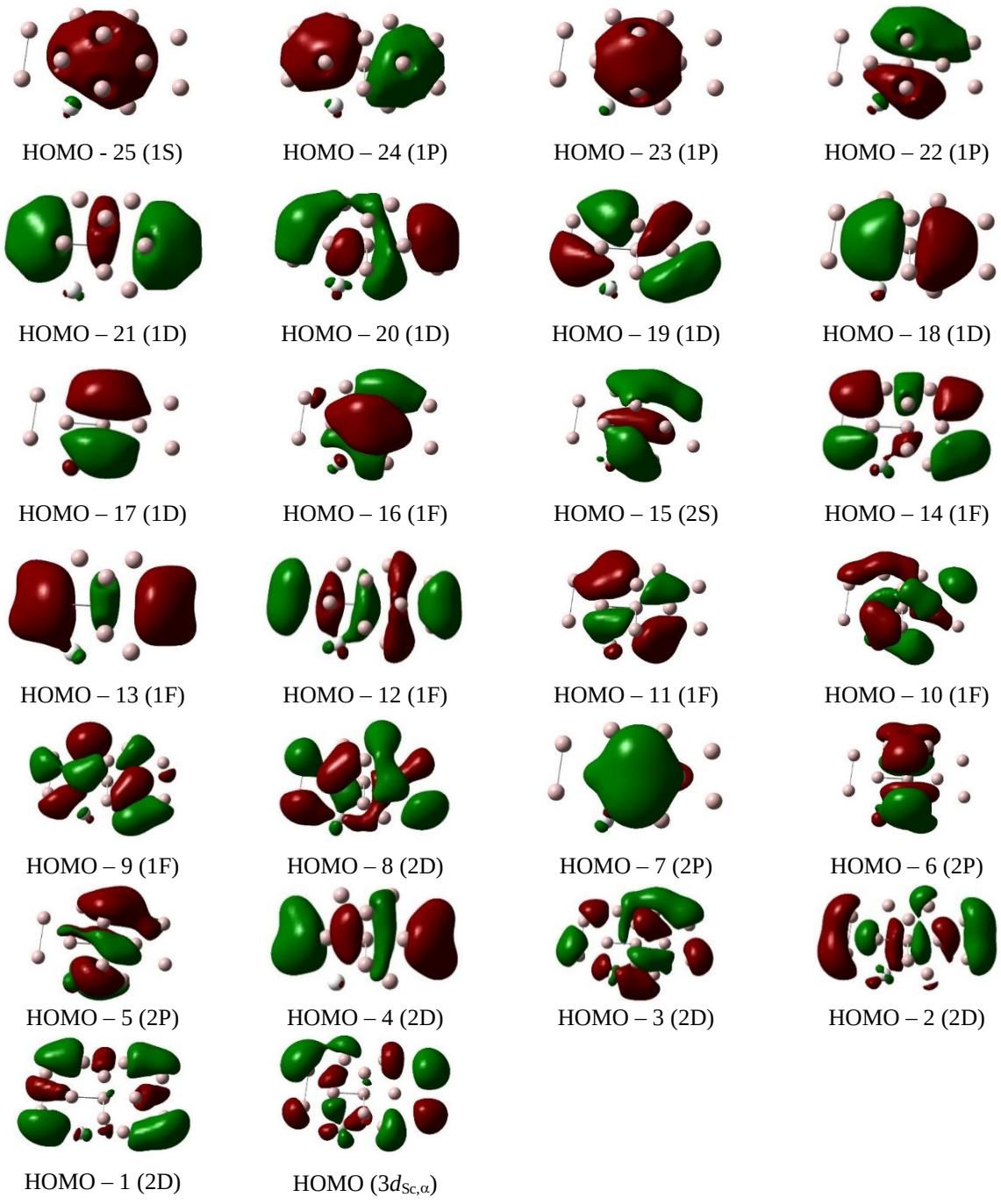

Figure 4. Images of several frontier orbitals of the $Al_{16}Sc$ cluster.

$Al_{16}Sc$ and $Al_{16}Sc^+$

Let us now describe in some detail the electronic configurations of the neutral $Al_{16}Sc$ clusters (M=Sc). Each Al atom in $Al_{16}M$ contributes three valence electrons, whereas the Sc atom contributes also two to its cluster shell and keeps one valence electrons in its orbital. The number of valence

electrons contributed by the constitution atoms to the cluster shell amounts to 50 that occupy thus 25 shell MOs. By carrying out inspection of the images of several frontier MOs of the $Al_{16}Sc$ cluster, we have come to the assignment of electron configuration of the $Al_{16}Sc$ cluster, which is $\left[1S^2 1P^6 1D^{10} 1F^2 2S^2 1F^{12} 2D^2 2P^6 2D^8\right] 3d^1_{Sc,\alpha}$.

Of the 51 valence electrons, 50 electrons form a closed shell and there is only 1 unpaired electron of localized mainly on the 3*d*(Sc) atomic orbital, outside of the shell MOs. This statement is further confirmed when we compare this electron configuration with that of the $Al_{16}Sc^+$ cationic cluster, being $1S^2 1P^6 1D^{10} 1F^2 2S^2 1F^{12} 2D^2 2P^6 2D^8$. The 50-electron shells are completely preserved in both clusters, as the transition of electron configuration from the neutral to the cationic form takes place mainly on the outside of the MO shell, where there is an unpaired electron of the Sc atom. In addition to that, we also studied the change in charge of the Sc atom in the two forms, namely neutral and cationic clusters, and found that this value varies significantly, with - 0.6 in the neutral form and - 0.2 in the cationic form.

$Al_{16}Ti$ and $Al_{16}Ti^{2+}$

The $Al_{16}Ti$ has 52 valence electrons, as each Al atom contributes three and the Ti contributes four valence electrons into the shell of molecular orbitals.

Again, by carrying out inspection of the images of several frontier MOs of the $Al_{16}Ti$ cluster, the electron configuration of the $Al_{16}Ti$ has been assigned, being $\left[1S^2 1P^6 1D^{10} 1F^2 2S^2 1F^{12} 2D^2 2P^6 2D^8\right] 3d^1_{Ti,\alpha} 3d^1_{Ti,\alpha}$

From calculations it is found that of the 52 valence electrons of $Al_{16}Ti$ neutral cluster, 50 electrons form a stable shell alike that of $Al_{16}Sc$ and the remaining two unpaired electrons localize mainly on 3*d*(Ti) atomic orbitals. As comparing the electron configuration of the $Al_{16}Ti$ neutral with that of the $Al_{16}Ti^{2+}$ cationic cluster, it is realized that the 50 valence electrons is unchanged.

After studying two pairs of clusters $Al_{16}Sc$ and $Al_{16}Sc^+$, $Al_{16}Ti$ and $Al_{16}Ti^{2+}$, we continue to learn the sequence of the electron configuration of the remaining clusters based on the inspection of images of the frontier MOs of other investigated clusters, namely the $Al_{16}V$, $Al_{16}Cr$, $Al_{16}Mn$, $Al_{16}Fe$, $Al_{16}Co$, $Al_{16}Ni$, $Al_{16}Cu$, and $Al_{16}Zn$ clusters. The results of the electron configuration of the clusters from $Al_{16}Cr$ to $Al_{16}Zn$ are summarized in the Table 2.

From Table 2 one can see that, apart from the *3d* electron in the outer shell, most of these clusters have similar shell electronic configuration of the 50 valence electrons which is almost the same as the previously analyzed clusters. Specifically, the two clusters, $Al_{16}Mn$ and $Al_{16}Zn$, are different from the other clusters as the two clusters have half-filled and full-filled *3d* subshell, respectively.

Table 2. The electron configuration of the clusters from $Al_{16}Cr$ to $Al_{16}Zn$

Cluster	Electron configuration
$Al_{16}Cr$	$\left[1S^2 1P^6 1D^{10} 1F^2 2S^2 1F^{12} 2D^2 2P^6 2D^8\right] 3d^1_{Cr,\alpha} 3d^1_{Cr,\alpha} 3d^1_{Cr,\alpha} 3d^1_{Cr,\alpha}$
$Al_{16}Mn$	$\left[1S^2 1P^6 1D^8 1F^2 1D^2 2S^2 1F^{12} 2D^2 2P^6 2D^8\right] 3d^1_{Mn,\alpha} 3d^1_{Mn,\alpha} 3d^1_{Mn,\alpha} 3d^1_{Mn,\alpha} 3d^1_{Mn,\alpha}$
$Al_{16}Fe$	$\left[1S^2 1P^6 1D^{10} 1F^2 2S^2 1F^{12} 2D^2 2P^6 2D^8\right] 3d^2_{Fe} 3d^1_{Fe,\alpha} 3d^1_{Fe,\alpha} 3d^1_{Fe,\alpha} 3d^1_{Fe,\alpha}$
$Al_{16}Co$	$\left[1S^2 1P^6 1D^{10} 1F^2 2S^2 1F^{12} 2D^2 2P^6 2D^8\right] 3d^4_{Co} 3d^1_{Co,\alpha} 3d^1_{Co,\alpha} 3d^1_{Co,\alpha}$
$Al_{16}Ni$	$\left[1S^2 1P^6 1D^{10} 1F^2 2S^2 1F^{12} 2D^2 2P^6 2D^8\right] 3d^6_{Ni} 3d^1_{Ni,\alpha} 3d^1_{Ni,\alpha}$
$Al_{16}Cu$	$\left[1S^2 1P^6 1D^{10} 1F^2 2S^2 1F^{12} 2D^2 2P^6 2D^8\right] 3d^8_{Cu} 3d^1_{Cu,\alpha}$
$Al_{16}Zn$	$1S^2 1P^6 1D^{10} 2S^2 1F^2 d^{10}_{Zn} 1F^6 2P^2 1F^4 2P^4 2D^{10}$

3.4. Magnetic Moments

When a pure aluminum cluster is doped by a transition metal atom, the outer most orbitals of the impurity including *d* and *s* shell can combine with the valence orbitals of the host to form shell orbitals of the resulting doped clusters. For the studied $Al_{16}M$, the valence electrons of the metal will combine to build up its magnetic moment. Fig. 5 indicates the change in the total magnetic moment (TMM) value of the neutral $Al_{16}M$ clusters as M goes from Sc to Zn. The perception of how the total and local magnetic moments of the clusters arise can be confirmed in considering the calculated values of local magnetic moments on each constituent atoms of the clusters that are displayed in Table 3. The total magnetic moment of the $Al_{16}M$ increases steadily from $1\mu_B$ for the Sc dopant to the maximum value $5\mu_B$ for the Mn dopant, then decreases to $0\mu_B$ for the Zn dopant.

As shown in Table 3, the magnetic moments of $Al_{16}M$ clusters are mostly held on the transition metal atoms, being 0.4, 1.8, 3.4, 4.6, 4.5, 3.0, and 1.8 for the Sc, Ti, V, Cr, Mn, Fe, and Co dopants, respectively. Remarkably, in spite of possessing high total spin magnetic moment, being $2\mu_B$, the total magnetic moment of $Al_{16}Ni$ is delocalized over aluminum atoms instead of nickel atom and this reveals that the magnetism of the Ni impurity atom is quenched in the endohedral doped structure $Al_{16}Ni$.

Table 3. Total magnetic moment (TMM, μB) and local magnetic moment (LMM, μB) of each atom of $Al_{16}M$ clusters

LMM	$Al_{16}Sc$	$Al_{16}Ti$	$Al_{16}V$	$Al_{16}Cr$	$Al_{16}Mn$	$Al_{16}Fe$	$Al_{16}Co$	$Al_{16}Ni$	$Al_{16}Cu$
Al (1)	0.1	0.0	0.0	0.0	0.0	0.0	0.0	0.1	0.0
Al (2)	0.0	0.0	0.0	0.0	0.0	0.0	0.0	0.0	0.0
Al (3)	0.0	0.0	0.0	0.0	0.0	0.0	0.0	0.0	0.0
Al (4)	0.0	0.0	0.0	0.0	0.0	0.0	0.0	0.1	0.0
Al (5)	0.0	0.0	0.0	0.0	0.0	0.0	0.0	0.0	0.0
Al (6)	0.0	0.0	-0.1	0.0	0.0	0.1	0.1	0.0	0.0
Al (7)	0.0	0.0	0.0	0.0	0.0	0.0	0.1	0.1	0.0
Al (8)	0.0	0.0	0.0	0.0	0.0	0.0	0.0	0.0	0.0
Al (9)	0.0	0.0	0.0	0.0	0.0	0.0	0.0	0.0	0.0
Al (10)	0.0	0.0	0.0	0.0	0.0	0.0	0.0	0.0	0.0
Al (11)	0.0	0.0	-0.1	-0.1	0.1	0.1	0.1	0.0	0.1
Al (12)	0.0	0.0	-0.1	-0.3	0.3	0.5	0.4	0.4	0.5
Al (13)	0.3	0.0	-0.1	-0.2	0.1	0.2	0.3	0.4	0.3
Al (14)	0.0	0.0	0.0	0.0	0.0	0.0	0.1	0.4	0.0
Al (15)	0.2	0.2	0.0	0.0	0.0	0.0	0.0	0.4	0.0
Al (16)	0.0	0.0	0.0	0.0	0.0	0.1	0.1	0.1	0.1
M (17)	0.4	1.8	3.4	4.6	4.5	3.0	1.8	0.0	0.0
TMM	1.0	2.0	3.0	4.0	5.0	4.0	3.0	2.0	1.0

4. Conclusions

The geometric and electronic structures, stability, and magnetic properties of the aluminum cluster doped with first-row 3*d* transition metal atoms, $Al_{16}M$ (M = Sc, Ti, V, Cr, Mn, Fe, Co, Ni, Cu, and Zn), have been investigated within the framework of the density functional theory. The calculated results indicate that the neutral $Al_{16}M$ cluster are stabilized at three kind of structures, including two exohedral doped isomers and one endohedral doped structure. There is a competition between the endohedral and the exohedral structures of $Al_{16}M$ with M being Ni, Cu, and Zn. The most stable structure of $Al_{16}Ni$

prefers the endohedral shape while the endohedral and the exohedral structures for both $Al_{16}Cu$ and $Al_{16}Zn$ are energetic degenerate within small energy gaps of lower 0.1 eV. DFT calculations showed that the endohedral structure $Al_{16}Ni$ gets the highest value for both average binding energy and embedded energy as compared to the remaining $Al_{16}M$ counterparts while the calculated values of ionization energy indicate that the transition metal doping reduces the ionization potential of the pure aluminum clusters. According to NBO calculations, the total magnetic moment of $Al_{16}M$ steadily increases from 1μB for Sc doping to a maximum value of 5μB for Mn doping, and then steadily decreases down to 0μB for Zn doping. Remarkably, the calculated results of local magnetic moment reveal that the magnetism of the encapsulated Ni dopant is quenched in Al_{16} cage. Furthermore, NBO analyses, also utilized to examine the electronic structures of $Al_{16}M$, show that the 50-electron shells are completely preserved in both clusters $Al_{16}Sc$ and $Al_{16}Ti$ and the remaining unpaired electron(s) localize(s) mainly on 3*d* atomic orbitals of metal dopant.

Acknowledgments

This research is funded by Vietnam National Foundation for Science and Technology Development (NAFOSTED) under grant number 103.01-2019.372.

References

[1] W. A. D. Heer, The Physics of Simple Metal Clusters: Experimental Aspects and Simple Models, Rev. Mod. Phys, Vol. 65, Iss. 3, 1993, pp. 611, https://doi.org/10.1103/RevModPhys.65.611.

[2] M. B. Knickelbein, Experimental Observation of Superparamagnetism in Manganese Clusters, Phys. Rev. Lett., Vol. 86, Iss. 23, 2001, pp. 5255-5257, https://doi.org/10.1103/PhysRevLett.86.5255.

[3] P. G. Reinhard, E. Suraud, Introduction to Cluster Dynamics, Wiley-VCH, Weinheim, 2004.

[4] F. Baletto, R. Ferrando, Structural Properties of Nanoclusters: Energetic, Thermodynamic, and Kinetic Effects, Rev. Mod. Phys., Vol. 77, Iss. 1, 2005, pp. 371, https://doi.org/10.1103/RevModPhys.77.371.

[5] R. Ferrando, J. Jellinek, R. L. Johnston, Nanoalloys: from Theory to Applications of Alloy Clusters and Nanoparticles, Chem. Rev., Vol. 108, No. 3, 2008, pp. 845-910, https://doi.org/10.1021/cr040090g.

[6] J. Jia, J. Z. Wang, X. Liu, Q. K. Xue, Z. Q. Li, Y. Kawazoe, S. B. Zhang, Artificial Nanocluster Crystal: Lattice of Identical Al Clusters, Appl. Phys. Lett., Vol. 80, 2002, pp. 3186, https://doi.org/10.1063/1.1474620.

[7] P. J. Roach, W. H. Woodward, A. W. Castleman, A. C. Reber, S. N. Khanna, Complementary Active Sites Cause Size-Selective Reactivity of Aluminum Cluster Anions with Water, Science, Vol. 323, Iss. 5913, 2009, pp. 492-495, https://doi.org/10.1126/science.1165884.

[8] P. Jena, Q. Sun, Super Atomic Clusters: Design Rules and Potential for Building Blocks of Materials, Chem. Rev., Vol. 118, Iss. 11, 2018, pp. 5755, https://doi.org/10.1021/acs.chemrev.7b00524.

[9] F. C. Chuang, C. Wang, K. Ho, Structure of Neutral Aluminum Clusters Al_n ($2 \leqslant n \leqslant 23$): Genetic Algorithm Tight-Binding Calculations, Phys. Rev. B, Vol. 73, Iss. 12, 2006, pp. 125431. https://doi.org/10.1103/PhysRevB.73.125431.

[10] B. K. Rao, P. Jena, Evolution of the Electronic Structure and Properties of Neutral and Charged Aluminum Clusters: A Comprehensive Analysis, J. Chem. Phys., Vol. 111, Iss. 5, 1999, pp. 1890-1904, https://doi.org/10.1063/1.479458.

[11] O. P. Charkin, D. O. Charkin, N. M. Klimenko, A. M. Mebel, A Theoretical Study of Isomerism in Doped Aluminum XAl_{12} Clusters (X=B, Al, Ga, C, Si, Ge) with 40 Valence Electrons, Chem. Phys. Lett., Vol. 365, Iss. 5-6, 2002, pp. 494-504, https://doi.org/10.1016/S0009-2614(02)01512-9.

[12] N. M. Tam, L. V. Duong, N. T. Cuong, M. T. Nguyen, Structure, Stability, Absorption Spectra and Aromaticity of The Singly and Doubly Silicon Doped Aluminum Clusters $Al_nSi_m^{0/+}$ with n = 3–16 and m = 1, 2, RSC Adv, Vol. 9, Iss. 47, 2019, pp. 27208, https://doi.org/10.1039/C9RA04004H.

[13] M. Wang, X. Huang, Z. Du, Y. Li, Structural, Electronic, and Magnetic Properties of a Series of Aluminum Clusters Doped with Various Transition Metals, Chem. Phys. Lett., Vol. 480, Iss. 4-6, 2009, pp. 258-264, https://doi.org/10.1016/j.cplett.2009.09.027.

[14] A. Varano, D. J. Henry, I. Yarovsky, DFT Study of H Adsorption on Magnesium-Doped Aluminum Clusters, J. Phys. Chem. A, Vol. 114, Iss. 10, 2010, pp. 3602-3608, http://dx.doi.org/10.1021/jp911013t.

[15] A. Pramann, A. Nakajima, K. Kaya, Photoelectron Spectroscopy of Bimetallic Aluminum Cobalt Cluster Anions: Comparison of Electronic Structure and Hydrogen Chemisorption Rates, J. Chem. Phys., Vol. 115, Iss. 12, 2001, pp. 5404, https://doi.org/10.1063/1.1394944.

[16] C. L. Dufaure, C. Blanc, G. Mankowski, C. Mijoule, Density Functional Theoretical Study of Cu_n, Al_n (n = 4–31) and Copper Doped Aluminum Clusters: Electronic Properties and Reactivity with Atomic Oxygen, Surf. Sci., Vol. 601, Iss. 6, 2007, pp. 1544-1553, http://dx.doi.org/10.1016/j.susc.2007.01.015.

[17] T. Sengupta, S. Das, S. Pal, Transition Metal Doped Aluminum Clusters: an Account of Spin, J. Phys. Chem. C, Vol. 120, Iss. 18, 2016, pp. 10027-10040, https://doi.org/10.1021/acs.jpcc.6b00510.

[18] X. Li, A. E. Kuznetsov, H. F. Zhang, A. I. Boldyrev, L. S. Wang, Observation of All-Metal Aromatic Molecules, Science, Vol. 291, Iss. 5505, 2001, pp. 859-861, https://doi.org/10.1126/science.291.5505.859.

[19] X. Li, H. Zhang, L. Wang, A. E. Kuznetsov, N. A. Cannon, A. I. Boldyrev, Aromatic Mercury Clusters in Ancient Amalgams, Angew. Chem., Vol. 40, Iss. 18, 2001, pp. 3369-3372, https://doi.org/10.1002/1521-3773(20010917)40:18<3369:AID-ANIE3369>3.0.CO;2-Z.

[20] G. X. Ge, Y. Han, J. G. Wan, J. J. Zhao, G. H. Wang, The Role of TM's (M's) d Valence Electrons in $TM@X_{12}$ and $M@X_{12}$ Clusters, J. Chem. Phys., Vol. 6, 2013, pp. 125123, https://doi.org/10.1063/1.4973636.

[21] B. Fan, G. X. Ge, C. H. Jiang, G. H. Wang, J. G. Wan, Structure and Magnetic Properties of Icosahedral Pd_xAg_{13-x} (x = 0–13) Clusters, Sci. Rep., Vol. 7, 2017, pp. 9539, https://doi.org/10.1038/s41598-017-10184-6.

[22] Y. Li, N. M. Tam, A. P. Woodham, J. T. Lyon, Z. Li, P. Lievens, A. Fielicke, M. T. Nguyen, E. Janssens, Structure Dependent Magnetic Coupling in Cobalt-Doped Silicon Clusters, J. Phys. Chem. C, Vol. 120, Iss. 34, 2016, pp. 19454, https://doi.org/10.1021/acs.jpcc.6b06320.

[23] G. X. Ge, H. X. Yan, J. M. Yang, L. Zhou, J. G. Wan, J. J. Zhao, G. H. Wang, Manipulation of Magnetic Anisotropy in Ir_{n+1} Clusters by Co Atom, Phys. A Stat. Mech. Appl., Vol. 453, 2016, pp. 194-202, https://doi.org/10.1016/j.physa.2016.02.050.

[24] E. Janssens, S. Neukermans, P. Lievens, Shells of Electrons in Metal Doped Simple Metal Clusters, Current Opinion in Solid State and Materials Science, Vol. 8, Iss. 3-4, 2004, pp. 185-193, https://doi.org/10.1016/j.cossms.2004.09.002.

[25] R. Pal, L. F. Cui, S. Bulusu, H. J. Zhai, L. S. Wang, X. C. Zeng, Probing the Electronic and Structural Properties of Doped Aluminum Clusters: MAl−12 (M=Li, Cu, and Au), J. Chem. Phys., Vol. 128, Iss. 2, 2008, pp. 024305, https://doi.org/10.1063/1.2805386.

[26] E. J. Izal, D. Moreno, J. M. Mercero, J. M. Matxain, M. Audiffred, G. Merino, J. M. Ugalde, Doped Aluminum Cluster Anions: Size Matters, J. Phys. Chem. A, Vol. 118, Iss. 24, 2014, pp. 4309-4314, https://doi.org/10.1021/jp501496b.

[27] V. Kumar, Y. Kawazoe, Hund's Rule in Metal Clusters: Prediction of High Magnetic Moment State of $Al_{12}Cu$ From First-Principles Calculations, Phys. Rev. B, Vol. 64, Iss. 11, 2001, pp. 115405, https://doi.org/10.1103/PhysRevB.64.115405.

[28] X. Xia, Z. G. Zhang, H. G. Xu, X. Xu, X. Kuang, C. Lu, W. Zheng, Geometric Structures and Electronic Properties of $Al_nV^{0/-}$ (n = 5–14) Clusters: Photoelectron Spectroscopy and Theoretical Calculations, J. Phys. Chem. C, Vol. 123, Iss. 3, 2019, pp. 1931, https://doi.org/10.1021/acs.jpcc.8b09010.

[29] S. M. Lang, P. Claes, S. Neukermans, E. Janssens, Cage Structure Formation of Singly Doped Aluminum Cluster Cations Al_nTM^+ (TM = Ti, V, Cr), J. Am. Soc. Mass Spectrom., Vol. 22, Iss. 9, 2011, pp. 1508-1514, https://doi.org/10.1007/s13361-011-0181-1.

[30] Y. Hua, Y. Liu, G. Jiang, J. Chen, Minimal Size of Endohedral Singly Vanadium-Doped Aluminum Cluster: a Density-Functional Study, Eur. Phys. J. D, Vol. 67, 2013, pp. 267, https://doi.org/10.1140/epjd/e2013-40306-0.

[31] Y. Hua, Y. Liu, G. Jiang, J. Du, J. Chen, Geometric Transition and Electronic Properties of Titanium-Doped Aluminum Clusters: Al_nTi (n = 2–24), J. Phys. Chem. A, Vol. 117, Iss. 12, 2013, pp. 2590, https://doi.org/10.1021/jp309629y.

[32] Y. Hua, Y. Liu, J. Chen, DFT Studies on Geometrical Structures, Stabilities, and Electronic Properties of AlnCr(n = 1-24) Clusters, Eur. Phys. J. Plus, Vol. 133, 2018, pp. 524, https://doi.org/10.1140/epjp/i2018-12302-9.

[33] N. T. Cuong, N. T. Mai, N. T. Tung, N. T. Lan, L. V. Duong, M. T. Nguyen, N. M. Tam, The Binary Aluminum Scandium Clusters Al_xSc_y with x + y = 13: When is the Icosahedron Retained?, RSC Adv., Vol. 11, Iss. 63, 2021, pp. 40072, https://doi.org/10.1039/D1RA06994B.

[34] M. J. Frisch, H. B. Schlegel, G. E. Scuseria, M. A. Robb, J. R. Cheeseman, J. A. Montgomery et al., Gaussian 09 Revision: D.01, 2009.

[35] N. E. Schultz, G. Staszewska, P. Staszewski, D. G. Truhlar, Validation of Theoretical Methods for the Structure and Energy of Aluminum Clusters, J. Phys. Chem. B, Vol. 108, Iss. 15, 2004, pp. 4850-4861, https://doi.org/10.1021/jp0370223.

[36] Y. Ouyang, J. Wang, Y. Hou, X. Zhong, Y. Du, Y. Feng, First Principle Study of AlX (X = 3d,4d,5d Elements and Lu) Dimer, J. Chem. Phys., Vol. 128, 2008, pp. 074305, https://doi.org/10.1063/1.2831506.

[37] H. T. Pham, L. V. Duong, B. Q. Pham, M. T. Nguyen, The 2D-to-3D Geometry Hopping in Small Boron Clusters: The Charge Effect, Chem. Phys. Lett., Vol. 577, 2013, pp. 32-37, https://doi.org/10.1016/j.cplett.2013.05.041.

[38] M. Saunders, Stochastic Search for Isomers on a Quantum Mechanical Surface, J. Comput. Chem., Vol. 25, Iss. 5, 2004, pp. 621, https://doi.org/10.1002/jcc.10407.

[39] A. Aguado, J. M. López, Structures and Stabilities of Al_n^+, Al_n, and Al_n^- (n=13–34) Clusters, J. Chem. Phys., Vol. 130, Iss. 6, 2009, pp. 064704, https://doi.org/10.1063/1.3075834.

[40] Q. A. Smith, M. S. Gordon, Electron Affinity of Al_{13}: a Correlated Electronic Structure Study, J. Phys. Chem. A, Vol. 115, Iss. 5, 2011, pp. 899, https://doi.org/10.1021/jp109983x.